A Methodology for Mapping Shrub Canopy Cover in the Great Basin Desert using High Spatial Resolution Satellite Imagery

Mary E. Cablk, Ph.D.
Christopher Kratt

July 2007

Publication No. 41236

prepared by

Desert Research Institute, Nevada System of Higher Education

prepared for

U.S. Department of the Interior

THIS PAGE INTENTIONALLY LEFT BLANK

EXECUTIVE SUMMARY

The Great Basin is the largest desert in North America and is topographically characterized by a general north-south trend of basins and mountain ranges. It is defined both floristically and hydrographically. Substantial quantities of groundwater are stored in aquifers beneath the basins of eastern Nevada and parts of western Utah. These basins are underlain by thick sequences of Paleozoic carbonate strata and support shrub-steppe vegetation. Estimating the stores of groundwater in the deep carbonate aquifer systems is important to stakeholders who have an interest in activities that require water, such as urban development.

Groundwater storage is largely controlled by recharge through precipitation that infiltrates the aquifer and the subsequent discharge of groundwater through seeps and springflow. Perhaps most significant in the discharge regime in arid and semi-arid environments is evapotranspiration by phreatophytic shrubs, which are defined by their ability to draw or discharge groundwater out of the system. Greasewood (*Sarcobatus vermiculatus*), is a commonly observed phreatophyte in the Great Basin, although sagebrush and other species are also known to use groundwater. Phreatophyte roots are able to access deeper stores of water when soil moisture from precipitation is not available. The draw of water from the subsurface followed by release of water vapor into the atmosphere through plant tissue is the process of transpiration. Together the draw of groundwater by phreatophytic vegetation and the loss of water from the interstitial soil are called *evapotranspiration.* The amount of groundwater that is discharged through the process of evapotranspiration can be a significant draw on water resources that may otherwise more deeply infiltrate an aquifer. For this reason, detailed estimates of phreatophytic vegetation extent, density, and phenology play an important role in the accurate estimation of groundwater discharge in a water budget.

High spatial resolution satellite imagery (~ 1 m spatial resolution) was used to map individual shrubs in the phreatophytic zone of 11 basins in eastern Nevada and western Utah. Spatial data sets of percent canopy cover were generated from this shrub map layer. Canopy cover was calculated, rather than estimated, to spatially match Landsat 28.5 m resolution and the hydrographically defined basins of the study area. This report describes the methodology developed for mapping individual shrubs using Space Imaging IKONOS data. Imagery was acquired on multiple dates over areas within a defined phreatophyte boundary for selected basins in the central Great Basin desert. Individual shrub canopies were identified based on spectral response of the IKONOS imagery and a binary (two class) data set of individual shrub locations was generated using supervised classification methods. The resulting shrub map layer was evaluated using quantitative accuracy assessment methods and found to have an overall accuracy of 84%, with a slight underestimation of shrubs. This methodology can be employed for mapping other shrub-dominated ecosystems and produce a data set that is useful in many different applications due to its thematic simplicity.

THIS PAGE INTENTIONALLY LEFT BLANK

CONTENTS

LIST OF FIGURES

LIST OF TABLES

INTRODUCTION

This study is one element of a regional analysis that is a joint effort between the Desert Research Institute and the U.S. Geologic Survey (USGS). The Basin and Range Carbonate Aquifer System (BARCAS) study was initiated by Congress in December 2004 with the purpose of estimating groundwater storage under selected areas of eastern Nevada and western Utah (Section 131 of the Lincoln County Conservation, Recreation, and Development Act of 2004; short title, Lincoln County Land Act). Under this legislation the Desert Research Institute and USGS in cooperation with the Utah State Engineers Office identified the following objectives: 1) Evaluate geohydrologic characteristics within the study area including the extent, thickness, and hydrologic properties of aquifers; volume and quality of water stored in aquifers; delineation of subsurface geologic structures controlling ground-water flow; ground-water flow direction and gradients; distribution of recharge and discharge areas; and representative rates of recharge and discharge; 2) Integrate geologic, hydrologic, and geochemical information to determine basin and regional ground-water budgets; and 3) Synthesize and evaluate all geohydrologic data to develop a three-dimensional conceptual description of the ground-water flow system. These data will be used to create a unified data-collection network for the study area.

Paramount to these efforts is the completion of a water budget, which includes estimates of groundwater discharge and recharge. This report more specifically addresses one discharge component, i.e., the groundwater draw within the phreatophyte zones of the study area. In many cases, the deciduous shrub "greasewood" (*Sarcobatus vermiculatus)* is used synonymously with the term "phreatophyte"; however we define phreatophytes according to Naumburg *et al*. (2005), defined as any semiarid shrub species that can use groundwater opportunistically during any time of the year, e.g., facultative. Facultative phreatophytes will use soil water from precipitation when it is available and easily obtainable. Therefore, the phreatophyte zone is considered to be those areas that are dominated by greasewood, but can and does also include other land cover types including sagebrush (*Artemesia tridentata)*, playa, agriculture, or grasslands within the zone matrix. Phreatophyte transpiration is a principle mechanism of groundwater discharge in arid and semiarid regions (Robinson, 1958; Nichols, 1993, 1994, 2001; Reiner *et al*., 2002; Nagler *et al*., 2005). Uncertainty in the estimates of groundwater discharge can lead to errors in water budget estimates. Few studies have been conducted in the Great Basin that quantify the contribution of phreatophytic vegetation groundwater use to total groundwater discharge (Nichols, 1993, 1994, 2001; Laczniak *et al*., 2001; Reiner *et al*., 2002). However, because vegetation covers most of the area where the groundwater table is accessible by phreatophyte root systems, accurately delineating the extent and percent cover of phreatophytic vegetation can significantly improve the discharge estimates of a water budget.

The amount of vegetation cover is typically categorized or estimated based on the fractional area of vegetation that occupies a grid cell, polygon, or other area of interest. Two parameters that comprise 'cover' include the horizontal density and the leaf area index (LAI), which is the number of leaf layers of the vertical density (Jiang *et al*., 2006). Evapotranspiration is controlled by both of these parameters, driven by the plant's ability to photosynthesize and its access to available soil moisture. Estimating vegetation cover over large areas has been a focal point in the remote sensing community since the launch of satellites and public availability of resulting data. Numerous sensors launched by several countries with various spatial scales from meters to kilometers have been coupled with multiple spectral and radiometric resolutions to study vegetation extent, phenology, productivity, succession, pattern, and a host of other phenomena. Yet extent of vegetation cover and specifically percent canopy cover has only been derived indirectly and this is due primarily to the limitations of the satellite sensors relative to the size of the vegetation. The spectral response of a landscape surface within one picture element (pixel) is an averaged value for a particular bandwidth over a typically heterogeneous area. Consequently the spectral response within a pixel is sensitive to both the configuration of the features within the pixel space as well as the composition of those features that affect absorption, reflectance and emittance in the electromagnetic spectrum (EMS). At a 30 m spatial resolution such as Landsat Thematic Mapper (TM), the recorded pixel value is a mean value over the corresponding landscape surface. Within that pixel on the landscape are a variety of elements, some of which are shrubs, some may be annual grasses or forbs, some may be bare soil or rocks, and some might be water or other cover types including shadow. Therefore correlating or otherwise relating a vegetation index value to a particular feature such as productivity, biomass, or greenness by default includes all of the features on the surface, not just the phreatophytes or necessarily the shrub vegetation.

Classification, empirical modeling, and transformation of vegetation indices have been the main tools available for deriving vegetation cover estimates either in whole or as part of a more comprehensive categorical description. The normalized difference vegetation index (NDVI) is arguably the most studied vegetation index in the remote sensing literature. NDVI has been correlated with LAI, fractional vegetation cover, vegetation condition, and biomass. Yet, the scientific literature is full of discrepancies on the issue of relationship between NDVI and fractional vegetation cover (Jiang *et al*., 2006). In semi-arid and arid areas where vegetation density is low and soil backgrounds dominate the spectral response, vegetation indices have been reported to perform poorly (Elvidge and Chen 1995). Other studies have reported positive relationships between NDVI and vegetation in semi-arid landscapes corresponding with seasonal precipitation patterns. Weiss et. al. (2004) reported positive results for potentially assessing vegetation variability in response to climate variability using time series NDVI. Again, pixel responses to rainfall include not only shrub vegetation but also cryptobiotic soil and other landscape elements so the increase and decrease in landscape response is based on a composite of features, not only shrub vegetation. Fractionating the composite elements of evapotranspiration, which are evaporation from soil, transpiration of soil moisture, and transpiration of groundwater, is very difficult if not impossible at a resolution greater than that of individual shrubs or shrub complexes.

The Great Basin Desert

The Great Basin Desert is the largest desert in North America. Most of Nevada and parts of western Utah and southern Oregon and Idaho are within the Great Basin Desert (Figure 1) which lies between the Sierra Nevada and the Rocky Mountains (Pellant *et al*, 2004). Considered a cold desert (Snyder *et al*, 2004), the plant communities in more mesic areas are dominated by the evergreen shrub *Artimisa tridentata* (Sagebrush) and in the lower more arid reaches of the valleys by salt desert shrub communities. Sagebrush is known to have a broad ecological tolerance and has adapted to be efficient in water uptake and retention (Taylor, 1992). Within the mesic sagebrush extent the deciduous shrub *Sarcobatus* *vermiculatus* (Greasewood) is also found and is thought to occur where depth to groundwater is less than 40 feet. Rabbitbrush species (*Chrysothamnus*) and *Atriplex* species such as hopsage (*Atriplex spinosa*) also occur intermixed in the greasewood and sagebrush communities.

Figure 1. The Great Basin Desert (heavy dashed outline) is the largest North American Desert and covers most of Nevada and parts of Utah, Oregon and Idaho.

Greasewood is well adapted to alkaline soils and tolerates salts more than other shrubs, allowing it to thrive along the playa-upland boundary. Grasses and forbs common to greasewood and sage communities also occur in the study area. The amount, type and distribution of forbs are highly dependent on amount and seasonality of rainfall. These annuals are not known to have the root structure or depth that would allow them to draw upon groundwater and are thus not considered to be phreatophytic.

STUDY AREA

Figure 2 outlines the individual basins that are found within the BARCAS study area and also shows areas that fall within the phreatophyte boundary and are covered by the IKONOS data. The study area typically receives an average of 253 mm of precipitation annually (Desert Research Institute, Western Region Climate Center). Mean annual maximum temperature over the past 30 years is 21.1º C and the mean annual minimum temperature is -8.3º C. Mean minimum temperatures in the winter months (December, January, February) average -7.5º C, while maximum temperatures in the summer months (June, July, August) average 19.8º C. There is variability among the study area basins, although in general the climate and weather patterns across the entire study area are consistent within the individual basins.

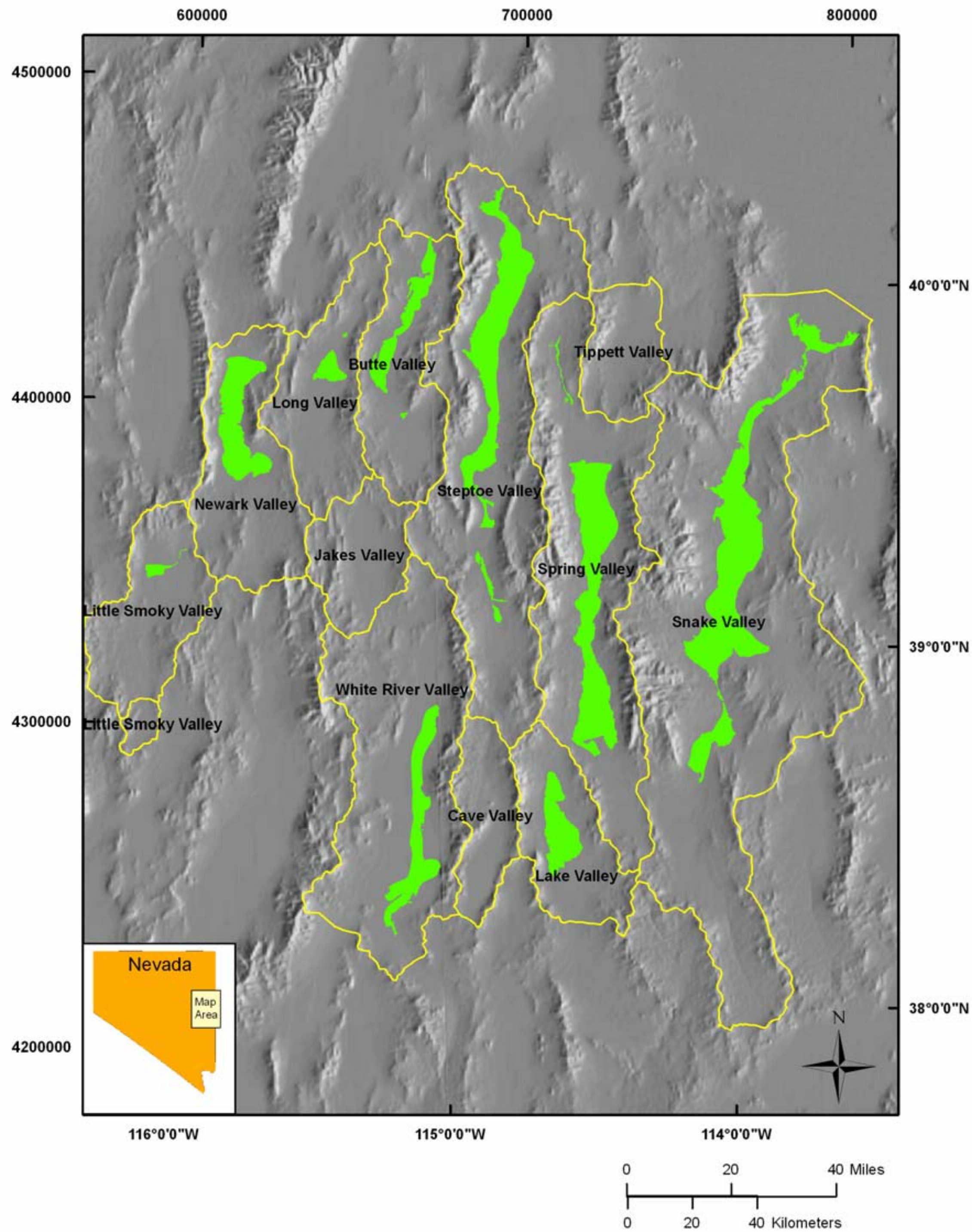

Figure 2. Shaded topographic relief image overlain with the location of basins within the BARCAS study area (yellow outline) and areas within the phreatophyte boundary and covered by IKONOS data shown in green (UTM zone 11 NAD83).

A phreatophyte boundary was provided by the U.S. Geologic Survey Water Resources Division based on reconnaissance studies conducted in the 1960's that identified greasewood vegetation as the extent of phreatophytes. This boundary file was used to identify the extent of satellite imagery required. Space Imaging acquires rectangular swaths of imagery but customers may submit digital shapes files for use as cookie-cutters to minimize purchase of unwanted imagery. In this manner the imagery purchased most closely approximates the user's area of interest and for this study our area of interest was the phreatophyte zones. An updated phreatophyte boundary was then provided by the USGS after the imagery was ordered and acquired. This updated boundary was mapped based on a variety of input sources including existing spatial data layers, aerial photographs, helicopter mapping efforts and more recent field site visits. In addition, the updated boundary was delineated to represent the potential area in which regional groundwater use by phreatophytes would be expected and the vegetation is dominated by greasewood (Laczniak, pers. comm., February 17, 2006). We used the intersection of the two phreatophyte boundary files for our focal study area. Because the revised boundary was provided after the imagery had been ordered there were some unavoidable data gaps. Merging the two boundaries was the best solution for working in the most recently delineated extent of phreatophytes although these boundaries have not been field validated. The total area we analyzed was approximately 352,807 ha over nine valleys (Table 1).

Table 1. Area of phreatophytic vegetation by valley for the BARCAS study area.

Valley Name	Hectares	Acres
Butte	18,664	46,120
Lake	20,692	51,130
Little Smokey	2,298	5,679
Long	5,534	13,675
Newark	32,709	80,826
Snake	105,368	260,370
Spring	71,183	175,895
Steptoe	64,646	159,742
White River	37,714	78,366
Total	358,808	745,568

IKONOS Imagery

The Space Imaging IKONOS (Thornton, Colorado, USA) sensor was the world's first commercial satellite to collect panchromatic (black-and-white) imagery at 1 m spatial resolution and multispectral imagery at 4-m spatial resolution. The satellite orbits the earth every 98 minutes at an altitude of 680 km (423 miles). It is in a sun-synchronous orbit that passes over the BARCAS study area at approximately 10:30 AM local time. The satellite can produce replicate images over the same geographic area every three days. IKONOS bands, 1, 2, and 3 correspond to visible blue, green and red light, respectively, while Band 4 corresponds to near-infrared wavelengths. Table 2 lists some of the technical details of the IKONOS instrument.

Table 2. IKONOS spectral and spatial resolution specifications.

Band	Wavelength range (µm)	Spatial resolution
Panchromatic	0.45 to 0.90	1 m
1	0.445 to 0.516	4 m
2	0.506 to 0.595	4 m
3	0.632 to 0.698	4 m
4	0.757 to 0.853	4 m

IKONOS imagery for the study area basins were acquired between Sept. 5^{th} and Dec. 10^{th}, 2005. The imagery was rectified in UTM zone 11 NAD83 for those scenes acquired over Nevada and in UTM zone 12 NAD83 for those scenes acquired over Utah. The positional accuracy of the images has a circular error with 90% confidence (CE90) at 4 m spatial resolution. This is equivalent to the U.S. National Map Accuracy Standard (NMAS) of 1:4,800. A total of 41 scenes of over 90 gigabytes of calibrated reflectance data were purchased to achieve coverage of the areas of interest.

High spatial resolution imagery was purchased for this project because canopy cover can be mapped at a 1-m spatial resolution after the multispectral data are fused with the panchromatic. Landsat Thematic Mapper (TM) or Landsat Enhanced Thematic Mapper (ETM+) both have a spatial resolution of approximately 30-m which is not fine enough to discriminate and identify individual shrub canopies. The spectral resolution of Landsat sensors includes data collected in the short-wave infrared (SWIR), which is useful for vegetation mapping but without the fine spatial resolution did not fulfill the mapping objectives of this project. Even the 10-m spatial resolution of the French SPOT satellite is not adequate for such detailed mapping. Although aerial photographs can achieve the 1-m or finer spatial resolution, acquiring, processing and interpreting aerial photographs for the study area were both cost and time prohibitive. Furthermore, the process of orthorectification, which would be necessary to achieve the necessary ground control, would render the photographs unusable for spectral image processing. Satellite platforms, relative to aerial platforms, are stable and the data acquired from satellites can be rectified in a manner that maintains the spectral and radiometric integrity of the imagery while achieving desired or required ground control.

IKONOS bands are well suited for vegetation discrimination. Band 3 is centered on 0.65 µm, while Band 4 is centered on 0.85 µm. This configuration takes advantage of visible light absorbed by chlorophyll near 0.68 µm, juxtaposed by high vegetation reflectance in the near-infrared region (Goetz *et al*., 1983). The continuum between these two wavelength regions is commonly referred to as the red-edge. This reflectance characteristic is somewhat unique and particularly strong for healthy vegetation and is the spectral feature that allows vegetation to be distinguished from other non-living surface cover types, such as rock, open water, and bare soil. Differences in red-edge reflectance can be observed among different vegetation types and therefore used to group vegetation into separate classes. A more detailed discussion about the image processing for shrub mapping is provided in the next section.

Methods

Figure 3 diagrams the overall process for mapping shrub locations from the IKONOS reflectance data to final product. Each of 41 images was separately processed from fusing to final shrub layer. Fusing the 1-m spatial resolution panchromatic band with the 4-m multispectral data capitalized on the full spatial and spectral information provided by IKONOS. The fused imagery was then subset to focus the analyses within the phreatophyte boundary only, thus simplifying the processing and eliminating superfluous data outside the area of interest. The imagery was transformed using algorithms designed to maximize differentiation of landscape elements such as vegetation, soil and water. We used the Tasseled Cap Transformation (Horne, 2003) and describe this process in detail in a following section. Within the transformed data, shrubby areas were identified and a classifier was trained to group all areas with similar statistical properties throughout the image. The resulting product was reviewed and refined as necessary until a suitably accurate representation of the shrub cover was achieved.

Fusing

The purpose of fusing the 4-m and 1-m IKONOS data was to extract the detail of the spatial information in the 1-m panchromatic band and merge it with the spectral information of the 4-m multispectral data. There are numerous methods for fusing different spatial resolution data, including but not limited to highpass filtering (Chavez, 1986), intensity-hue-saturation (IHS) (Carper *et al*., 1990), and Brovey transform (Tu *et al*., 2005). Because IKONOS data are 11-bit it is critical to maintain the radiometric integrity through the fusion transformation process. Reducing the data from 11-bit to 8-bit significantly reduces the variation in spectral reflectance as the range possible of values changes from 2048 to 256, respectively, and can therefore potentially homogenize what would otherwise be diagnostic differences in reflectance. The IHS, Brovey transform and multiplicative method (MULTI) reduce the original data integrity which is problematic for subsequent analyses (Svab and Ostir, 2006). Principal component analysis (PCA) is an orthogonal statistical process that transforms multivariate data onto new and uncorrelated axes. PCA maintains 11-bit resolution whereas other fusion methods do not. The objective of PCA is to maximize variance within the entire data set while maintaining spatial integrity. The resulting data set was an 11-bit image at 1-m spatial resolution in the visible and near-infrared bands.

Masking

To reduce computational time for the entire set of 41 images, a mask for each fused file was constructed based on the phreatophyte boundary. The mask function essentially eliminates all data outside of the area of interest. Here, the area of interest is only those areas within the phreatophyte boundary. By masking the data, extraneous data that are not part of the study area were eliminated from processing and subsequent analysis. This also decreased the amount of processing time and reduced the overall file sizes. Masking the data was necessary because the original phreatophyte boundary used to specify the imagery extent was updated after the imagery was acquired. Because the two boundaries differed in extent it was necessary to mask the imagery to the final area of interest in this case the intersection of the two phreatophyte boundaries.

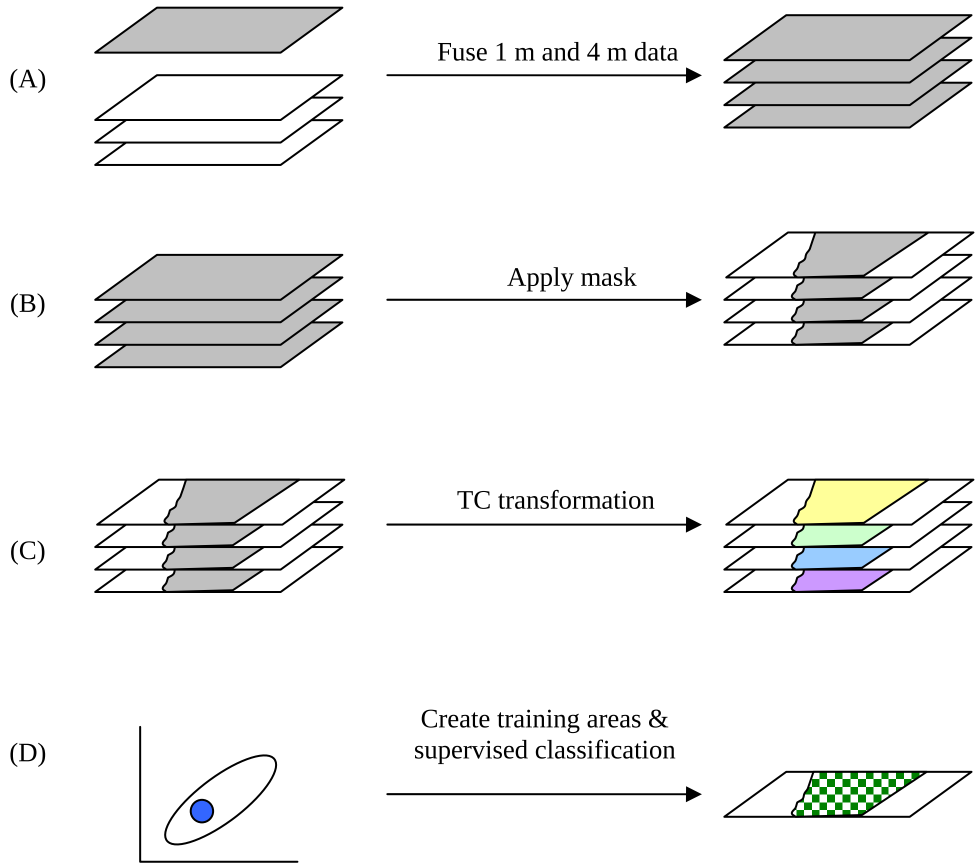

Figure 3. Overall processing of imagery begins with (A) with fusion of the 1-m and 4-m data; followed by (B) masking the data precisely to the phreatophyte boundary; (C) transforming the fused, masked data using the Tasselled Cap and finally (D) selecting training areas in each scene for conducting the final supervised classification.

Supervised Classification

After these preparatory steps of fusing and masking the imagery were completed, the goal was to produce a shrub map layer that most accurately identified individual shrubs. We employed a supervised classification approach by taking advantage of red-edge features in IKONOS bands 3 and 4 as well as incorporating information from bands 1 and 2 at 1-m spatial resolution. The first step in the classification process was to run a Tasseled Cap (TC) transformation on each of the fused and masked files. The Tasseled Cap transformation (Horne, 2003) is an orthogonal linear transformation applied to each IKONOS band across the four band data set to maximize band-to-band variability within the highly correlated data. It is similar to Principal Component Analysis (PCA) except that the transformation is a universal set of equations. Therefore, the resulting feature space plots between any two bands are interpretable across any landscape (Jensen, 2005). Landscape cover types such as vegetation, soil, and water, are consistently found in known regions of 2-dimensional scatterplots regardless of the geographic location of the data set. The resulting TC transformed bands are known as 'brightness,' 'greenness,' 'wetness,' and 'non-such.' As their names imply, the first two TC bands enhance the inherent brightness and greenness characteristics, of the data respectively, and provide a more statistically separable and visually interpretable range of vegetation pixels. The latter two bands, which combined typically yield less than 5% of the data set variability, are not well understood. Hence, the shrub vegetation and background soils were classified using the combination of brightness and greenness TC bands for each of the images.

A band 4, 3, 2 composite image was displayed and interactively linked with a two-dimensional scatter plot of the TC brightness (y-axis) and greenness (x-axis) bands. Because of the high spatial resolution of the imagery, landscape features such as shrubs, anthropogenic features, and trees were readily apparent and visually identifiable. Therefore it was useful and expeditious to compare the transformed data with the original false-color infrared composites. Groups of pixels that corresponded to vegetation in the image were selected in the TC band scatter plot for development of training areas. Statistics from these pixels were then used in a parallelepiped (e.g., Jensen, 2005) supervised classification of the corresponding image using the same TC bands. This process was iterated several times after refining the pixel selection from the two-dimensional scatter plot and visually assessing the classified results against the band 4, 3, 2 composite image until an acceptable shrub map layer was achieved. The result from this iterative classification process was a two-class spatial data layer where each 1 m pixel was assigned either a '0' for no shrub or '1' for shrub. This process was separately applied to all 41 files. Dividing those pixels classified as shrub by the total area allowed a percent canopy cover estimate to be made for any size mapping unit.

Classification is an iterative process where parameters defining the training areas in spectral space are set, the classifier is run, evaluated, and if results are not acceptable the process is run again with altered input parameters. As part of this process, each resulting shrub map file was qualitatively assessed after all classification iterations. Characteristics of misclassified areas were noted and subsequent processing approaches were re-employed to improve the final canopy cover estimate. Despite this, certain land cover types were challenging to differentiate spectrally. Grasses in riparian and wetland areas were commonly misclassified as shrubs. Trees were also occasionally misclassified but were less problematic since few occur within the phreatophyte boundary. Sparse to moderately dense shrubs growing on a dark soil background also caused confusion in the classification and areas of dark soil had a tendency to be misclassified as shrub.

To improve the overall accuracy of the shrub map layer where class confusion existed but could not be resolved by spectral separation we manually created masks for trees, dark soils, riparian and wetland grasses by on-screen digitizing. Polygons were drawn to include areas that clearly were not shrub but were classified as shrub. These polygons were then applied as masks to the shrub data sets and those areas classified incorrectly as shrub were converted to a correct classification as non-shrub. Trees, riparian areas, and grasslands were straightforward to correct in this manner. The confusion between shrubs and these features were based on the limited bandwidth of the IKONOS sensor and its inability to distinguish between the reflectance of chlorophyll across different vegetation types and dark soils with microbiotic crusts. Broad contiguous areas of shrubs typically did not co-occur with these classes so applying manual masking techniques only served to increase the accuracy of the shrub layer data set. Separating areas of dark soil proved to be more challenging because there were often shrubs growing in dark soils. Large contiguous areas of dark soils were masked out if they were sparsely populated by shrubs. Otherwise, they were not excluded as this would inappropriately reduce the shrub classified area. After all of the 41 images were processed and final shrub map layers were complete for each image, the data sets were composited into one large file and treated as a regional data set for all analyses.

Accuracy Assessment

Quantitative accuracy assessments are critical particularly when the spatial data set will be used in further analyses, whether for simple calculation of extent of a land cover class or more sophisticated use in complex mathematical models. An accuracy assessment gives power to the user of a data set, in that a level of confidence for the data set can be articulated and used by land managers to make the most scientifically sound decisions. Accuracy assessments are quantitative and accepted methods are found in peer-review and academic literature for conducting rigorous calculations (Jensen, 2005; Stehman 2000; Congalton and Green, 1999; Thappa and Bossler 1992). Field work is typically required when suitably high spatial resolution data, such as videography, orthophotographs, or satellite imagery are not available or not in a format that can be used with geographic confidence. The shrub map layer was generated from very high spatial resolution IKONOS imagery and therefore the best accuracy assessment is the use of field validation methods.

The shrub map layer was considered to be one entire data set, not a series of basins, and therefore was accuracy assessed as a whole. The method employed was a stratified-random, systematic-clustered sampling procedure. Because time and cost are always issues with generating any reference data set, spatially random points were stratified to fall within 250 m of a road (paved, gravel, dirt, or 4x4 trail) and within public land. The number of random validation points needed for a statistically sound reference data set for the shrub map layer was calculated using Equation (1):

$$N = Z^2(p)(q) / E^2 \qquad (1)$$

where, N= the number of ground control points, Z = 2 (from the standard normal deviate of 1.96 for the 95% 2-sided confidence level), p = expected percent accuracy, q = 100-p, and E = allowable error. This is based on the formula for the binomial probability theory and as such is appropriate for a binary data set (0 or 1) such as this shrub map layer (Jensen, 2005; Congalton and Green, 1999). Based on an expected accuracy of 85%, which is generally considered acceptable in the remote sensing literature, and with an allowable error of 4%, a total of 319 points at a minimum were targeted. At each stratified-random location we followed a systematic-clustered sample regime where four data points were collected, one in each cardinal direction from the stratified-random location. This procedure was both statistically rigorous and field efficient.

Global positioning system (GPS) data were collected in the field to locate the reference points using a Tripod Data System with a Ranger data logger running Solo software. All GPS data were logged only when the GPS signals would result in a realtime differentially corrected coordinate within 0.5 m level accuracy. Because the shrub map layer was 1-m data within NMAS at 1:12,000 GPS coordinates collected were well within sufficient ground resolution. It was expected that the accuracy of the GPS would be higher than the rectified imagery, which would potentially bias the results of the confusion matrix. For this reason, data were collected at road intersections that are readily discernable in the imagery to assess the quality of the matched field reference data. The reference data were then co-registered to the imagery based on the ground control points to maximize co-registration between the GPS data and the imagery. Figure 4 provides an illustration of the data collected at each ground control point (GCP).

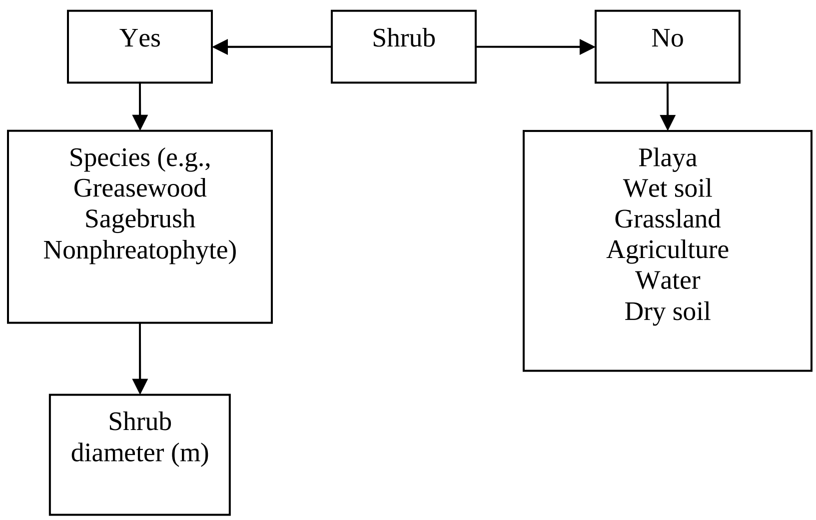

Figure 4. Data collection for reference data used in the accuracy assessment of the shrub map layer. At each location the presence of a shrub was recorded. If a shrub were present the species and shrub diameter were recorded. If the location did not contain a shrub, the land cover type was recorded.

The validation data file was designed so that the field data collected on the ground could be integrated into other assessments covering the same geographic area. At each validation point the location was recorded as having a shrub or no shrub, if a shrub was present the species was recorded and if a shrub was not present the land cover type was documented. At each GCP where there was a shrub, the diameter of the shrub or shrub cluster was measured and recorded as a continuous number. Individual shrub diameters were typically symmetric and therefore were recorded with a single measurement. Interstitial spaces were not typically symmetrical and therefore size could not be accurately captured. The challenge in referencing high spatial resolution imagery of ± 4-m spatial accuracy with differentially corrected GPS data of <1 m accuracy is the potential for misregistration between the image data and the ground GPS coordinates. It was not practical to perform additional rectification of the entire regional data set and the consistency of warp differences throughout and among the individual images contained within the single regional data set was not known. Therefore collecting points at center lines of roads close to reference points allowed in-place rectification of the reference GPS data to the single regional shrub map layer. Despite various levels of accuracy, some error exists in all rectified data sets. Therefore it was necessary to make some allowances for the difference in accuracy and precision between the shrub map layer and the reference data. Because of potential co-registration errors and the method of measuring shrubs while at the same time not measuring non-shrub spaces called for two levels of precision in the rule base criteria. The first level of precision required a pixel class value to match the GPS reference point value for the non-shrub case. This did not allow for any registration error to be accounted for, hence error in the non-shrub class was expected to be higher and was not quantifiable. The second level of precision took advantage of shrub sizes as a distance of measure from the center of the GPS reference point. If a shrub on the shrub map layer was within the measured distance it was regarded as a match to the reference data. This provided a correction for spatial registration errors between the highly accurate field GPS coordinates and the slightly less accurate image data set. An error matrix was generated to quantitatively compare the results of the field collected reference data with the IKONOS shrub map layer. Errors of omission, commission, overall accuracy, and two kappa coefficients of agreement were calculated for the data set to provide a complete accuracy assessment of the image-based shrub map layer.

RESULTS

Accuracy Assessment

A total of 347 validation targets were visited in the field from July 22 to August 2, 2006. As is standard practice, more random points were computer generated than required because unforeseen circumstances often arise in the field that result in exclusion of some points. The typical reason for exclusion is the lack of physical accessibility of computer selected verification points. All points that had been generated *a priori* and could physically be reached were included in the accuracy assessment, e.g., 347 of 365 points. The resulting overall accuracy of the shrub map layer was 84%. The error matrix generated from the reference and classified data set is provided in Table 3. Errors of omission and commission were calculated and also shown in Table 3. Shrubs were more likely to be missed (error of omission) rather than non-shrub areas incorrectly mapped as shrubs (error of commission). In this case these errors indicate that the data set somewhat under-represents shrub area. The kappa coefficient of agreement of 0.68 was calculated for the entire regional shrub map layer. The conditional kappa coefficient of agreement by class was 0.89 for shrub and 0.85 for non-shrub. The kappa coefficient of agreement is a measure of accuracy between the shrub map layer and the reference data accounting for chance assignment of pixels to a class. The closer the kappa is to a value of 1, the less likely the classification could be reproduced by random or chance class assignment. A kappa coefficient of 0.68 is at the high end of moderate accuracy, and therefore the image-based shrub cover data are unlikely the result of random assignment. The accuracy assessment provides quantitative support of the data quality that may be used to provide confidence levels for future modeling efforts. The conditional kappa eliminates the chance agreement from the calculation for each class and is an indicator of agreement or accuracy for each class individually. For shrubs the accuracy was 89% and for non shrubs 85%. Accuracy by class for each valley sampled is shown in Table 4. Two valleys were not sampled simply as a function of the rule base and random class generator; e.g., road and public land access. The total phreatophyte area in these two valleys was approximately 6% of the entire phreatophyte area and because the shrub map layer was treated as a whole and not as individual valleys we believe the lack of field verification in the two valleys is not problematic.

Table 3. Error matrix for the IKONOS derived shrub map layer at 1m spatial resolution.

		Field Validation		
	Class	Shrub	Not Shrub	Total
Map	Shrub	153	21	174
	Not Shrub	35	138	173
	Total	188	159	347

Overall accuracy = 84%

Error of omission	Error of commission
Shrub = 17%	Shrub = 12%
Not shrub = 13%	Not shrub = 20%

Table 4. Percent agreement between the IKONOS-generated shrub map layer and the ground reference data collected between July 22 and August 2, 2006. Shrub percent indicates the accuracy of the shrub class, non-shrub is the accuracy of non-shrub areas and number of points is the total number of reference points visited in that valley. Date is the date or range of dates for the IKONOS image acquisition.

Valley Name	Shrub (%)	Non-shrub (%)	Number of Points	Date (2005)
Butte	83	100	9	October
Lake			Not sampled	
Little Smokey			Not sampled	
Long	80	100	9	September
Newark	100	71	35	October
Snake	95	84	179	Sept-December[1]
Spring	80	80	20	October
Steptoe	68	69	35	September
White River	78	74	60	September

[1]A total of nine images were used to map the shrubs in Snake Valley. The dates of acquisition were earlier in the year at the north end and later in the year in the south. Two scenes were from September, one from October, three from November, and three from December.

Percent Canopy Cover

Percent canopy cover must be calculated over an area and cannot be assigned at a 1-m pixel resolution because the values will be either 0 or 100%. Within the extent of the IKONOS imagery for the phreatophyte boundaries, the percent canopy cover was calculated for each basin. Canopy cover was also calculated for a Landsat TM equivalent pixel size of 28.5-m using a statistical mean for each aggregated IKONOS pixel. The percent canopy cover was then estimated for each basin in the study area using the statistical mean of the Landsat equivalent percent canopy cover data. Table 5 shows the calculated percent canopy cover by valley based on the 1-m shrub data set and percent canopy cover calculated over the aggregated pixels. The mean canopy cover estimated using Landsat equivalent spatial resolution does not deviate from the total canopy cover calculated from the 1-m IKONOS derived data. Because the calculation of mean canopy cover based on Landsat-equivalent spatial resolution data was based on aggregation of binary data, standard deviation was also calculated. The standard deviation is a measure of the variability in the data about the mean and within each valley was very high. This indicates high spatial heterogeneity in canopy cover that would be difficult to effectively delineate from non-shrub cover signal in a mixed reflectance pixel at the 28.5-m spatial resolution.

Table 5. Mean canopy cover estimated from Landsat equivalent (28.5-m) derived percent canopy cover and canopy cover derived from IKONOS shrub map layer. Values are calculated over the extent of the phreatophyte boundary within the IKONOS imagery extent. Note the high standard deviations by valley indicating high spatial variability in percent cover over the landscape.

	Landsat equivalent at 28.5-m		1-m IKONOS shrub
Valley Name	Mean	Std. Dev.	Total
Butte	44.9	29.1	44.2
Lake	12	15.1	12
Little Smokey	8.3	15	8.4
Long	54.8	28.9	54.8
Newark	12.2	21.1	12.3
Snake	13.4	18.4	11
Spring	19.1	25.5	18.7
Steptoe	18.1	23	18.1
White River	26.3	26.7	26.3

DISCUSSION

The methodology was effective and efficient for producing an accurate 1-m shrub map layer for the study area. The shrub map slightly under-represents the total shrub cover for the study area based on the accuracy assessment, but the individual class accuracies were shown to be very good. Accuracies varied by valley (Table 4). Newark and Snake Valleys had the best correlation between shrubs and reference data, respectively, while Butte and Long Valleys had the best representation of non-shrubs, respectively. Steptoe Valley presented the biggest mapping challenge most likely due to a high prevalence of dark soils. The imagery over Steptoe Valley was acquired on September 5, 2005 and senescence can begin earlier in the year during drought or atypically hot conditions. The date of acquisition could have impacted our ability to differentiate canopies based on vegetation response that may have been at an early to intermediate level of senescence in that valley. The Steptoe Valley results had more error in comparison to Snake Valley where the imagery was acquired much later, primarily in November and December 2005. Therefore the later acquisition dates of the Snake Valley images may enhance classification accuracies (see Table 4). While it is possible to iteratively improve any map product, the IKONOS-derived shrub map layer derived for this report was shown to be one that can be used with confidence in further analyses and with quantitative knowledge of the error size and type. While there are areas of over- and under-estimation within the regional shrub map layer; all of the valleys visited had agreement indicating no single valley had unacceptable misclassification.

The implications of over- or under-estimation of the canopy extent relate directly to the discharge estimates that will be calculated across the study area. We found that overestimation occurred where there was confusion that could not be reconciled using either spectral or manual interpretation techniques. Grasses and dark soils were the two land cover types that produced these classification errors. Confusion with grasses was readily remedied using manual masking techniques while the dark soils posed a more difficult challenge to overcome. In some instances we were able to reconcile the dark soils-shrub mapping while in other instances, it was impossible to effectively differentiate between the two. These two factors are discussed in detail below.

Project and phonological time constraints affected the dates of image acquisition. Ideally, imagery for mapping vegetation is acquired in the late summer or early fall when shrubs remain green and are photosynthetically active, but grasses and other background vegetation have senesced. Similar research in the eastern Great Basin has found early to mid September imagery ideal for mapping phreatophytes but also showed success at mapping shrub extent into the late fall (Desert Research Institute, 2006). We found that late season imagery can be used to accurately map the shrubs in the phreatophyte zone of the eastern Great Basin of Nevada and that date of acquisition did not result in systematic reduction of accuracy. It is most likely that the discrimination success is due to the high spatial resolution where mixed pixels contain fewer features than coarser resolution imagery, such as Landsat TM. Landsat pixels are an averaged value over the landscape equivalent to between 820 and 900 IKONOS pixels. The ‘landscape’ at 1-m spatial resolution includes different feature signal contributions than a 28.5-m pixel and in the soil-shrub matrix of the study area perhaps there exists enough homogeneity to differentiate class cover types.

Overall this data set slightly underestimates shrub cover, which should be noted for analyses involving extrapolation of rates of ET using this data set. ET rates applied to shrub areas using this data set can be expected to represent a lower discharge than actual ET-based discharge rates. However, this reduction in discharge may be quantified based on the accuracy assessment results.

Grasses

The IKONOS bands 3 and 4 reflectance characteristics are very similar for healthy (green) shrubs, grasses, and trees. Therefore, healthy vegetation of any type generally fell within the same region of the two-dimensional scatter plot of the Tasseled Cap bands and indicated a lack of statistical separation. Healthy agricultural crops are the exception as they tended to display significantly higher near-infrared values compared to natural and non-irrigated vegetation. This issue of spectral resolution could potentially be solved by increasing the number of spectral channels over the same wavelength region and/or including channels in the short-wave infrared region (1.0 – 2.5 μm) however the bands available from commercial sensors at high spatial resolution cannot be further divided. It is also often possible to differentiate different plant species based on their phenology if sufficient images are purchased throughout an entire growing season. For example in the southernmost extent of the study area big sagebrush is evergreen throughout the growing season, greasewood can start to leaf out in May and begin to senesce in early September, while budsage and grasses senesce in July all within the same geographic area. Because the grasslands were visually quite obvious within the IKONOS images we purchased, while not always spectrally distinct from shrubs, the masking technique proved to be quite effective at eliminating misclassification between the grasses and shrubs (Figure 5).

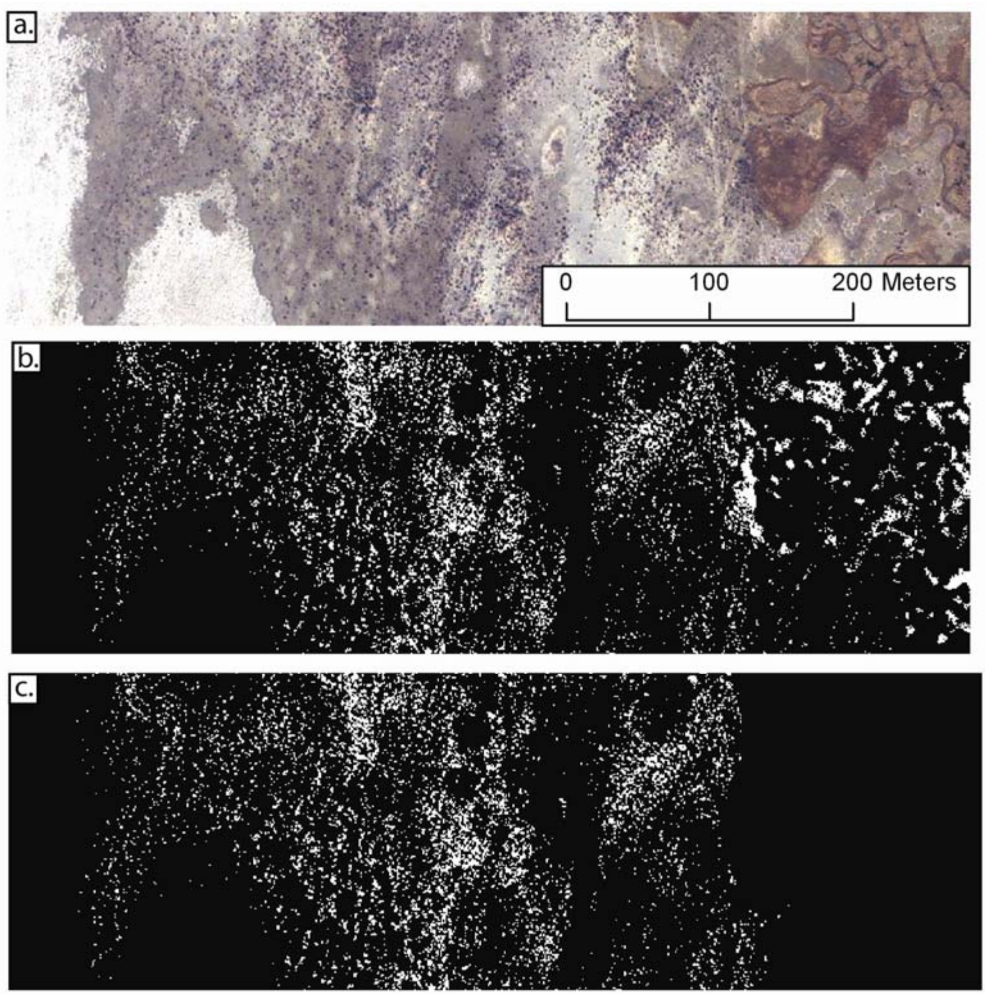

Figure 5. Comparison of images with the same spatial extent: (a) band 4,3,2 image; (b) with the unmasked shrub map layer showing false-positive marsh grasses on the right side of the image; and (c) and showing the manually masked version of the shrub map layer that excludes false-positives. Shrubs were identified as the white pixels in the binary (b) and (c) images.

Dark Soils

Close inspection of the data revealed that despite the Tasseled Cap transformation, dark soil backgrounds caused spectral ambiguity in areas where moderate to sparsely distributed shrubs coincide with dark soils. Because Landsat TM has routinely been used within the remote sensing community for vegetation analyses, we decided to compare the IKONOS data analysis results to the results that would have been achieved using the Landsat TM data. The problem of dark soil background interfering with vegetation discrimination in arid and semi-arid regions is well documented in the literature. Huete and Tucker (1991) discuss the problems of dark, high chroma soils which yield false 'greenness' similar to agriculture signals in arid regions. Vegetation indices are particularly susceptible to false classification through confusion with dark soils. This problem is pervasive throughout the U.S. southwest and across sensors. Qi *et al*. (1994) presented a Modified Soil Adjusted Vegetation Index (MSAVI) designed to maximize vegetation signal in regions with low vegetation density in an attempt to better discriminate vegetation from dark soils. The challenge with this index is that although it was developed for low to moderate canopy cover, it is based on cotton (*Gossypium hirsutum)*, an irrigated crop. The reflectance of cotton is much higher than native shrub-steppe species and therefore the results of the MSAVI applied to an irrigated agriculture crop represent a best case scenario. Elvidge and Chen (1995) found that nonlinear mixing of vegetation and background soils was most pronounced in broad-band sensors such as TM and Advanced Very High Resolution Radiometer (AVHRR). McGwire et al. (2000) found it took multiple sets of statistics to adequately separate all soil components from the shrubs in the Mojave Desert. Even with the fine spatial resolution of the IKONOS sensor, dark soils posed a challenge to extracting the vegetation signal in the work presented here. Soil properties for our study area are unlikely to change soon and are likely to be similar throughout the Great Basin at a regional level.

Because the research to date on vegetation mapping in the desert southwest has been done with moderate resolution imagery (i.e., > 5-m spatial resolution), we explored the dark soil properties of the IKONOS 1-m imagery in an attempt to better understand the source of the confusion between shrubs and dark soils. Figure 6 compares the average spectra from areas of mixed vegetation and dark soil, dark soil alone, and healthy dense vegetation. Although the mixed spectra and dark soil spectra do not appear to be closely matched, they are similar enough to commonly fall within the same region of a two-dimensional scatter plot. We overlaid the same polygons displayed Figure 6 (a-c) on a July 5, 2005 Landsat TM image and generated average spectra from this sensor for comparison (Figure 7). The spectral confusion is apparent in the Landsat imagery just as in the IKONOS imagery however the vector of confusion is different.

To ensure inclusion of low density shrubs on a dark soil background within the final shrub map layer, the regions-of-interest defined in the scatter plot and later used for supervised classification often encompassed the spectrally similar dark soil pixels and pixels with a dark soil/vegetation mixture. This led to the misclassification of dark soil pixels as shrub. Despite the misclassifications associated with dark soil in the IKONOS imagery, the high spatial resolution that allows direct canopy cover mapping also avoids spectral mixing problems that are more prevalent in coarser spatial resolution data sets where every pixel encompasses a mix of ground features. Even with 1-m data there still exists a spectral contribution from shadows. The opportunity for vegetation spectra to stand out against dark soil backgrounds would be optimized by acquiring IKONOS data sets acquired earlier in the growing season. However, as discussed above, other confusion between background vegetation including grasses, forbs and in particular exotics would swing the confusion as well.

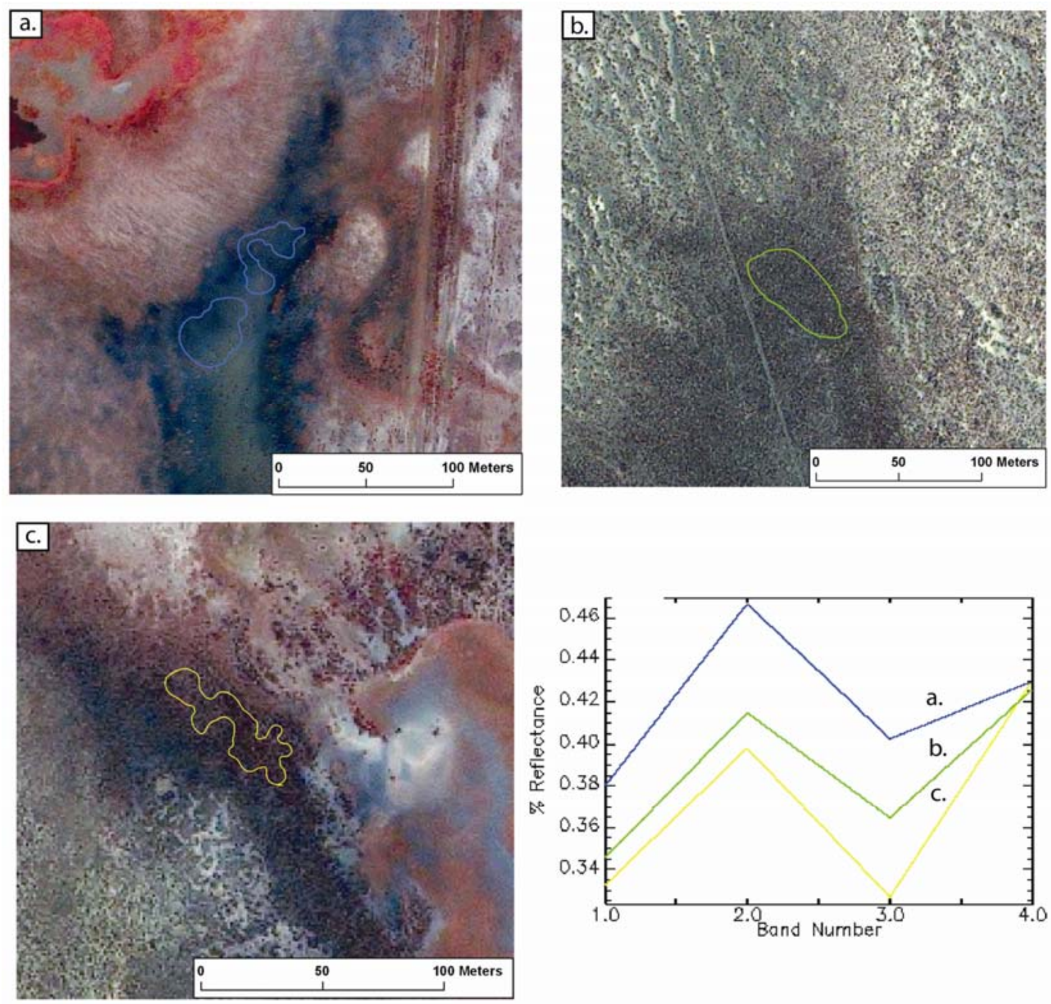

Figure 6. Comparison of averaged IKONOS color infrared images and averaged spectra from areas of (a) dark soil, (b) mixed vegetation and dark soil, and (c) dense healthy vegetation without dark soil background.

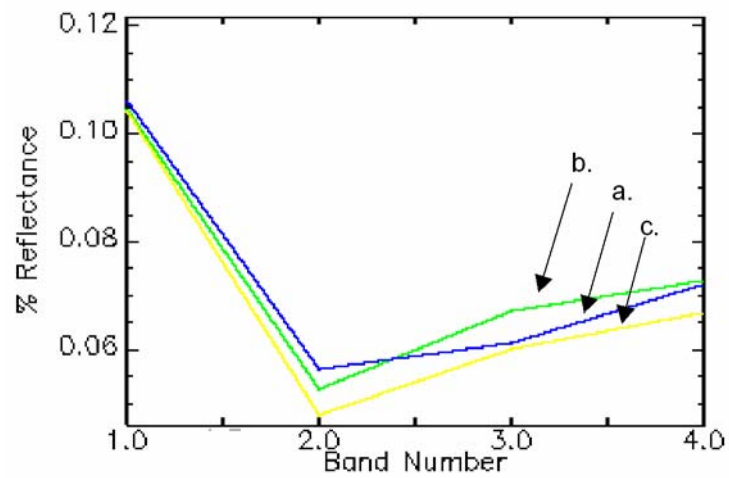

Figure 7. Averaged Landsat spectra corresponding to: (a) the dark soil; (b) mixed vegetation/dark soil; (b) and dense healthy vegetation areas shown in Figure 6.

Spectral mixing is less problematic with higher albedo, or brighter colored soils, due to a greater contrast ratio between the vegetation spectra and the soil spectra. Where the soils are brighter, pixels with a significant vegetation component are more readily identifiable and easy to group in two-dimensional plots. Figure 8 demonstrates a selected area where the background and vegetation were easy to spectrally differentiate, and therefore the shrubs could be accurately mapped. Confusion with other non-shrub vegetation is eliminated using masking techniques, resulting in just shrub and non-shrub delineations. This demonstrates the advantages of high spatial resolution imagery and its usefulness for creating data that maps shrubs, which may or may not be drawing groundwater depending on time of year and depth to groundwater.

CONCLUSIONS

The methodology developed for mapping shrubs from 1-m spatial resolution data is rigorous, accurate, repeatable, and provides a data set with quantified error useful for a diverse set of applications including modeling of basin-wide ET. There were challenges in differentiating targets in areas with dark soils and some spectral confusion occurred between different vegetation types during the growing season. However, the resulting classification has a quantified and acceptable accuracy which makes it far more useful for further analyses than an aggregate percent canopy cover data set derived from coarser spatial resolution imagery. Our comparison between Landsat-equivalent based percent canopy cover estimates (Table 5) demonstrated that the spatial variability inherent in the shrub landscape returns very large standard deviations at coarser spatial resolutions. Percent canopy cover can be calculated from the data set described in this report across scale and over almost any area of interest. This is inherently valuable compared to the limited utility of a categorical thematic canopy cover data set (i.e., classes of “low”, “medium”, “high”) comprised of density classes which cannot be refined to continuous (i.e., 0-100%) estimates. The canopy data set we developed could be used to refine an existing categorical classification into narrower classes. Most significantly, for the purposes of the BARCAS project, a more accurate representation of the extent of phreatophytic shrubs and the density of vegetation would enable refined estimates of groundwater discharge via evapotranspiration.

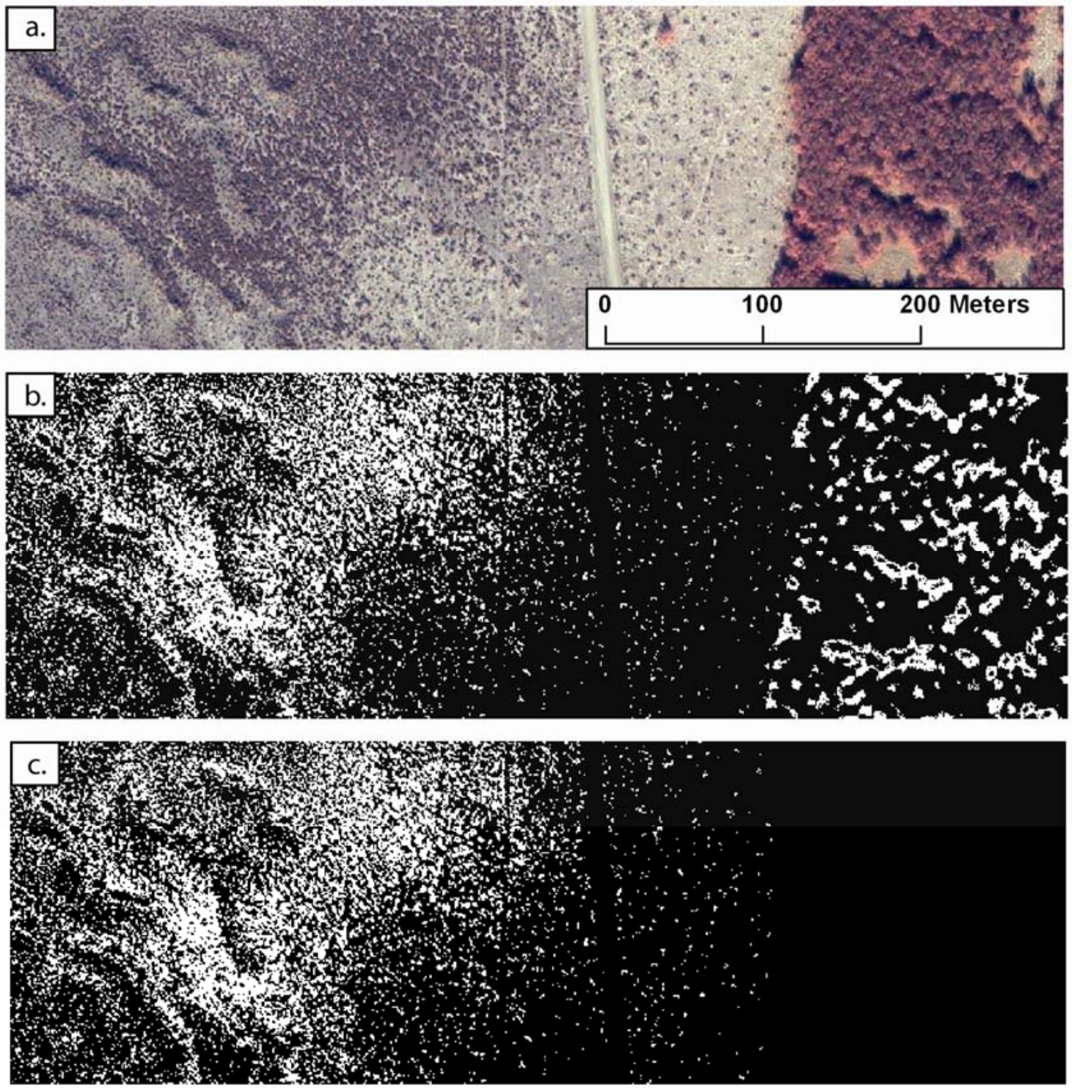

Figure 8. (a) comparison of band 4,3,2 image with (b) the resulting unmasked shrub map layer showing false-positive tree canopy edges on the right side of the image, and (c) showing the final manually masked version of the binary shrub layer that excludes false-positives. Shrubs are identified as the white pixels in the (b) and (c) binary images

REFERENCES CITED

Carper, W.J., T.M. Lillesand and R.W. Kiefer. 1990. The use of intensity-hue-saturation transformations for merging SPOT panchromatic and multispectral image data. *Photogrammetric Engineering and Remote Sensing.* 56(4):459-467.

Chavez, P.S. 1986. Digital merging of Landsat TM and digitized NHAP data for 1-24,000-scale image mapping. *Photogrammetric Engineering and Remote Sensing*. 52(10):1637-1646.

Congalton, R.G. and K. Green. 1999. Assessing the accuracy of remotely sensed data: Principles and Practices. Boca Raton, Fl. Lewis Publishers, 137 p.

Desert Research Institute, 2006. Evapotranspiration in Smoke Creek Desert, Nevada. DRI Publication No. 41224. 62 p.

Elvidge, C.D. and Z. Chen. 1995. Comparison of broad-band and narrow-band red and near-infrared vegetation indices. *Remote Sensing of Environment*. 54:38-48.

Goetz, F. H., and B. N. Rock, 1983. Remote sensing for exploration: an overview. Economic Geology, 78(4): 573-589.

Horne, J. H., 2003. A tasseled cap transformation for IKONOS imagery. ASPRS Annual Conference, Anchorage, AK.

Huete, A.R. and C.J. Tucker. 1991. Investigation of soil influences in AVHRR red and near-infrared vegetation index imagery. *International Journal of Remote Sensing*. 12(6):1223-1242.

Jensen, J.R., 2005. Introductory Digital Image Processing: a remote sensing perspective (3rd edition). Pearson Prentice Hall. Upper Saddle River, NJ.

Jiang, Z. A.R. Huete, J. Chen, Y. Chen, J. Li, G. Yan and X. Zhang. 2006. Analysis of NDVI and scaled difference vegetation index retrievals of vegetation fraction. *Remote Sensing of Environment.* 101:366-378.

Laczniak, R.J., J.L. Smith, P.E. Elliot, G.A. Demeo, M. Chatttigny, and G. Roemer, 2001. Ground-water discharge determined from estimates of evapotranspiration, Death Valley regional flow system, Nevada and California. U.S. Geological Survey Water-Resources Investigations Report 01-4195.

McGwire, K., T. Minor, and L. Fenstermaker. 2000. Hyperspectral mixture modeling for quantifying sparse vegetation cover in arid environments. Remote Sensing of Environment. 72(3):360-374.

Nagler, P.L., R.L. Scott, C. Westenburg, J.R. Cleverly, E.P. Glenn, and A.R. Huete. 2005. Evapotranspiration on western US rivers estimated using the Enhanced Vegetation Index from MODIS and data from eddy covariance and Bowen ration flux towers. *Remote Sensing of Environment*. 97:337-351.

Naumburg, E., R. Mata-Gonzalez, R.G. Hunter, T. McLendon, and D.W. Martin. 2005. Phreatophytic vegetation and groundwater fluctuations: A review of current research and application of ecosystem response modeling with an emphasis on Great Basin vegetation. *Environmental Management*. 35(6):726-740.

Nichols, W.D., 1993. Estimating discharge of shallow groundwater by transpiration from Greasewood in the Northern Great Basin. *Water Resources Research*, 29, 2771-2778.

Nichols, W.D., 1994. Groundwater discharge by phreatophyte shrubs in the Great Basin as related to depth to groundwater. *Water Resources Research,* 30, 3265-3274.

Nichols, W.D., 2001. Regional ground-water discharge by evapotranspiration and ground-water budgets, Great Basin, Nevada. U.S. Geological Survey Professional Paper 1628.

Pellant, M., B. Abbey, and S. Karl. 2004. Restoring the Great Basin Desert, USA: Integrating science, management, and people. *Environmental Monitoring and Assessment*. 99:169-179.

Qi, J. A. Chehbouni, A.R. Huete, Y.H. Kerr, and S. Sorooshian. 1994. A modified soil adjusted vegetation index. *Remote Sensing of Environment*. 48:119-126.

Reiner, S.R., R.J. Laczniak, G.A. Demeo, J.L. Smith, P.E. Elliot, W.E. Nylund, and C.J. Fridich, 2002. Ground-water discharge determined from measurements of evapotranspiration, other available hydrologic components, and shallow water-level changes, Oasis Valley, Nye County, Nevada. U.S. Geological Survey Water-Resources Investigations Report 01-4239.

Robinson, T.W., 1958. Phreatophytes: U.S. Geological Survey Water Supply Paper 1423.

Snyder, K.A., L.A. Donovan, J.J. James, R.L. Tiller, and J.H. Richards. 2004. Extensive summer water pulses do not necessarily lead to canopy growth of Great Basin and northern Mojave Desert shrubs. *Oecologia*. 141:325-334.

Stehman, S.V. 2000. Practical implications of design-based sampling inference for thematic map accuracy assessment. *Remote Sensing of Environment*. 72(1):35-45.

Svab, A. and K. Ostir. 2006. High-resolution image fusion: Methods to preserve spectral and spatial resolution. *Photogrammetric Engineering and Remote Sensing*. 72(5):565-572.

Taylor, R.J., 1992. Sagebrush Country: A wildflower sanctuary. Mountain Press Publishing Company. Missoula, MT.

Thappa, K. and J. Bossler. 1992. Accuracy of spatial data used in Geographic Information Systems. *Photogrammetric Engineering and Remote Sensing*. 58(6):835-841.

Tu, T.M., Y.C. Lee, C.P. Chang, P.S. Huang. 2005. Adjustable intensity-hue-saturation and Brovey transform fusion technique for IKONOS/QuickBird imagery. *Optical Engineering*. 44(11):Art. No. 116201.

Weiss, J.L., D.S. Gutzler, J.E.A. Coonrod, and C.N. Dahm. 2004 Long-term vegetation monitoring with NDVI in a diverse semi-arid setting, central New Mexico, USA. *Journal of Arid Environments*. 58(2):249-272.